ISBN: 978-3-95450-211-0 doi:10.18429/JACoW-SRF2019-MOP081

CONSIDERATIONS FOR EFFICIENT RF OPERATION FOR THE ADVANCED CW-LINAC DEMONSTRATOR AT GSI

C. Burandt[1,2*], K. Aulenbacher[1,2,4], W. Barth[1,2], M. Basten[3], M. Busch[3], F. Dziuba[1,2,4], V. Gettmann[1,2], M. Heilmann[2], J. List[1,2,4], S. Lauber[1,2,4], T. Kürzeder[1,2], M. Miski-Oglu[1,2], H. Podlech[3], A. Schnase[2], M. Schwarz[3], S. Yaramyshev[2]

[1]HIM Helmholtz Institute Mainz, 55099 Mainz, Germany
[2]GSI Helmholtzzentrum für Schwerionenforschung GmbH, 64291 Darmstadt, Germany
[3]IAP Goethe Universität Frankfurt, 60438 Frankfurt am Main, Germany
[4]KPH Johannes Gutenberg Universität Mainz, 55128 Mainz, Germany

Abstract

The FAIR@GSI accelerator facility will require the GSI-UNILAC to provide short heavy ion pulses of highest intensity at low repetition rate for injection into the 18-Tm-synchrotron SIS18. On the other hand, successful physics programs as for SHE (Super Heavy Elements) rely on the UNILAC (UNIversal Linear ACcelerator) providing for heavy ion beams of high average current and high duty factor. In the next future, a dedicated superconducting (SC) CW-Linac should therefore deliver CW beams to the experiments associated with those programs. As a first step towards this goal, beam tests with a single SC Cross-bar H-mode (CH) cavity were successfully conducted in 2017/2018. Within the scope of an Advanced Demonstrator project, current activities now aim for a beam test of a full cryomodule with three SC CH cavities and a SC rebuncher. Given a limited amount of RF power available per cavity and the necessity to accelerate different ion species with different mass-to-charge ratios, the loaded quality factor Q of the different resonators has to be chosen very carefully. This contribution discusses the simulations performed in this context.

INTRODUCTION

The UNILAC is a critical part of the injector chain for the future *Facility for Antiproton and Ion Research* (FAIR). Therefore, it is subject of ongoing optimization towards a short-pulsed, high-intensity, low-duty factor heavy ion LINAC which can utilize the full capability of the SIS18 synchrotron. While this optimization is in progress [1], today the UNILAC also serves different experiments with requirements, which are quite contrarious. Notable examples are the synthesis of Super Heavy Elements (SHE) [2] and material sciences. They rely on the UNILAC operated at variable beam energy and high average intensity. Preferably, the latter is realized by operating the accelerator in CW-mode. Furthermore, the UNILAC's beam time will be assigned to its role as an injector for SIS18 exclusively.

Superconducting radio-frequency (SRF) cavities facilitate compact design of CW accelerators and allow for high energy efficiency. The Helmholtz Linear Accelerator (HELIAC) is a SRF heavy ion accelerator which has been proposed to complement the existing and otherwise foreseen LINACs at GSI. Its purpose is to keep the SHE program and other activities, depending on the UNILAC today, competitive. In a joint effort with Helmholtz Institute Mainz (HIM) and under key support of Institut für Angewandte Physik (IAP) of Goethe University Frankfurt, the HELIAC is under development. The design comprises a dedicated ECR (Electron Cyclotron Resonance) ion source, a room temperature injector and twelve SRF cavities grouped into four cryomodules (see Fig. 1). Table 1 summarizes the design parameters.

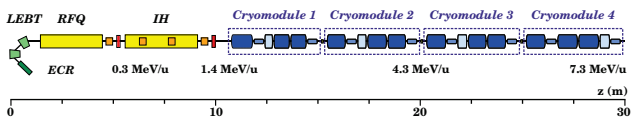

Figure 1: Layout of the HELIAC accelerator.

The project has already accomplished important milestones. In 2015 and 2016 cold tests of a prototype SRF structure (henceforth called CH0) proved the feasibility of the production of the complex superconducting Cross-bar H-mode (CH) cavities [3, 4]. During 2017 and 2018 the capability to accelerate heavy ion beams with the same cavity was demonstrated successfully [5–8].

Currently an *Advanced CW-Linac Demonstrator* is under development. It will comprise four superconducting cavities in a cryomodule which shall in future serve as the standard cryomodule for the HELIAC (see Fig. 2). Beside the proto-

Table 1: Design Parameters of the HELIAC [9] and the *Advanced CW-Linac Demonstrator* (Adv. Dem.)

	HELIAC	Adv. Dem.
A/q	≤ 6	≤ 6
f_0 (MHz)	216.816	
$I_{\mathrm{beam,\,max}}$ (mA)	1	1 (0.1)
E_{in} (MeV/u)	1.4	1.4
E_{out} (MeV/u)	3.5 – 7.3	2.7 – 3.3
ΔE_{out} (keV/u)	±3	*tbd*
# of SRF cavities	16	4

* c.burandt@gsi.de

ISBN: 978-3-95450-211-0 doi:10.18429/JACoW-SRF2019-MOP081

type cavity CH0, a re-buncher [10] (B1) and two short CH cavities (CH1 and CH2) will allow for increased output energies (compare 1). While not a limitiation of the cryomodule itself, the *Advanced CW-Linac Demonstrator* is going to be operated at 100 µA.

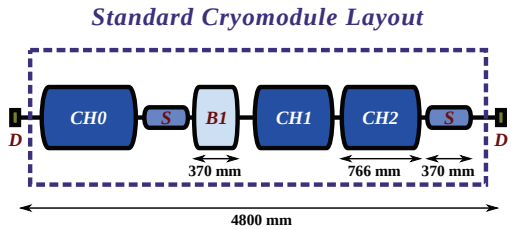

Figure 2: Layout of the Advanced Demonstrator cryomodule containing three CH cavities, a re-buncher cavity (B) and two solenoids (S).

The overall RF power efficiency of SRF-based acceleration depends heavily on the proper matching between amplifier and the cavity. For the above-mentioned beam test with CH0, a high power coupler was constructed. It is still subject of further development [11, 12]. During the tests a fixed coupling of $\beta_e \approx 2900$ [13] was used. This high value was chosen in order to relax the possible negative effect of microphonics and hence ease the first beam-related experiments at the expense of suboptimal power efficiency.

Critical parameters in this context are the fixed cavity properties Q_0, $[R/Q]$ and the variable acceleration voltage V_a as well as the beam parameters (current I_b and synchronous phase ϕ_s). Moreover, the amount and susceptibility of microphonics is an important issue. The peak detuning δf_{max} will severely influence the required amount of RF power. Since the HELIAC is intended as a universal accelerator with variable ouput energy and mass-to-charge ratio (A/q), the chosen matching will be a compromise and only be ideal for a single use case. For the *Advanced CW-Linac Demonstrator* it is intended to construct variable couplers [12]. Depending on the experience gained during this pre-project, the final HELIAC coupler will be designed to have a certain fixed coupling strength.

CH-CAVITIES

The HELIAC will be based on Cross-bar H-Mode (CH) cavities [14]. Table 2 shows the properties of the three different types that are going to be used in the *Advanced CW-Linac Demonstrator*. Notice however, that CH1, CH2 and B1 are still in production or under development and the given Q_0 cannot be regarded as final.

Table 2: Properties of the CH cavities [13, 15]

	CH0	CH1/2	B1
Frequency	— 216.816 MHz —		
# Gaps	15	8	2
Q_0	$> 1 \cdot 10^9$	$\gtrapprox 5 \cdot 10^8$	$\gtrapprox 5 \cdot 10^8$
$[R/Q]$	3240	1070	123

Figure 3: 3-D model of CH0 [3].

Figure 3 shows a 3-D model of CH0 which was used for structural mechanical analysis [16]. The pressure sensitivity is about 100 Hz/mbar. During production of CH0, prior to mounting the helium vessel around the cavity, a four-hour measurement of the momentary frequency deviation was carried out on a vertical test stand at 4 K. It showed a standard deviation of $\sigma = 2.1$ Hz, as shown in Fig. 4. Stable operation is considered to be possible when the RF system can compensate for a frequency deviation δf of at least 6σ. Since the mechanical mounting is quite different when the cavity is used for acceleration, an additional safety margin was applied, yielding $\delta f_{max} = 30$ Hz.

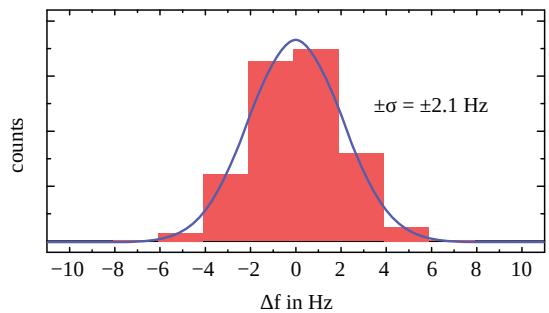

Figure 4: Result of a long-term measurement of the momentary frequency deviation of the CH0-Cavity (source: [3], modified).

BEAM DYNAMICS

Determination of RF power requirements presumes knowledge of the complex beam current, which the cavity is interacting with. The applied *Equidistant Multigap Structure* (EQUUS) beam dynamics concept allows for efficient acceleration between the equidistant gaps while maintaining a longitudinally stable bunch [17, 18]. Bunches enter the first gap of a cavity at a certain synchronous phase. As the velocity increases, the synchronous phase varies from gap to gap. In the HELIAC lattice, bunches typically enter the first gap of a cavity at a negative synchronous phase ϕ_s and leave with $\phi_s \approx 0$ or vice versa [19]. In the very long CH0 structure, the phase space trajectory starts with negative ϕ_s and will evolve to $\phi_s \approx 0$ for the center gaps and back to negative phases. Figure 5 illustrates this qualitatively. The net voltage presented by the cavity to the beam depends on both, the relative voltage in each gap (according to the field profile) and the synchronous phase. While the first is a fixed

ISBN: 978-3-95450-211-0 doi:10.18429/JACoW-SRF2019-MOP081

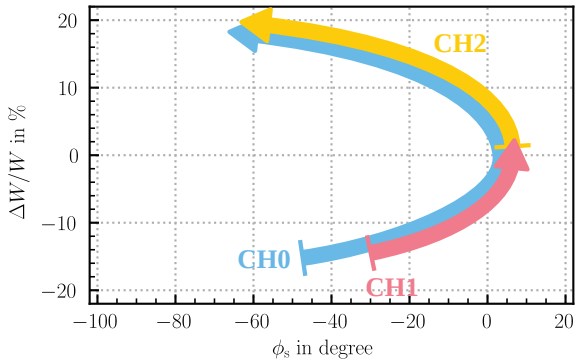

Figure 5: Simplified sketch of the possible evolution of the relative mean bunch energy and synchronous phase along the first cavities.

parameter, the latter is subject to the choices made during beam dynamical optimizations. It depends especially on the desired output energy. The following analysis of CH0 assumes an effective synchronous phase of ϕ_s between cavity voltage and beam current.

DETERMINING OPTIMAL COUPLING

RF Power Budget

Only part of the RF power provided by the amplifier of the RF system can be transferred to the beam. Figure 6 illustrates the breakdown of the power budget. Transmission line losses can be estimated to amount to 5 % to 10 %. Cavity wall losses range from few hundred mW to 10 W, depending on the selected accelerating voltage. Finally, the power delivered to the beam represents the useful fraction of the RF power initially invested.

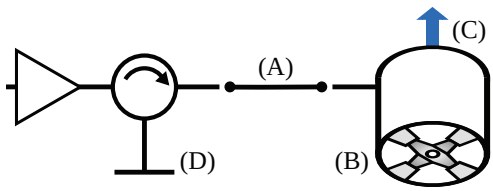

Figure 6: RF Power Budget: Transmission line losses (A), cavity wall losses (B), power transferred to beam (C), reflected power due to mismatches (D).

If the matching of the transmission line and the cavity is not perfect for a certain set of conditions (cavity and beam properties), another fraction of power is being reflected back towards the amplifier. While the cavity evidently failed to convert this power, it is still lost because it has to be dumped in a load before damaging the amplifier. While, in principle, the cavity can always be matched perfectly to any static beam, there are still losses to be expected because of microphonics. This dynamical detuning causes a momentary mismatch and therefore additional reflection of power.

Given a transmission line setup (characterized by length and loss per length), the SRF cavities (characterized by

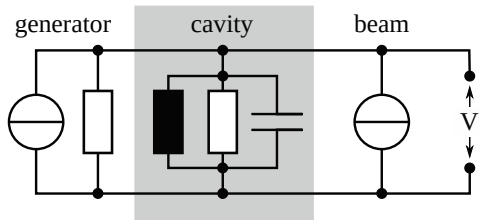

Figure 7: Equivalent circuit model as basis for the presented calculations.

$[R/Q]$ and Q_0) and certain beam parameters, only the reflected power remains to be manipulated in order to optimize the RF efficiency. This requires two parameters to be chosen: external coupling β_e and the amount of detuning of the cavity with respect to the RF reference frequency.

Optimal Coupling

The cavity and beam can be modeled as an equivalent circuit as shown in Fig. 7. Using circuit theory, the coupling of power to the beam can be derived [20].

Results for cavity CH0 are shown in Fig. 8. The plot on the top shows the required P_{fwd} for a cavity without beam loading as function of β_e and for different voltages (corresponding to different A/q). As expected, best matching is observed for $\beta_e = 1$. For the second plot, a beam current of

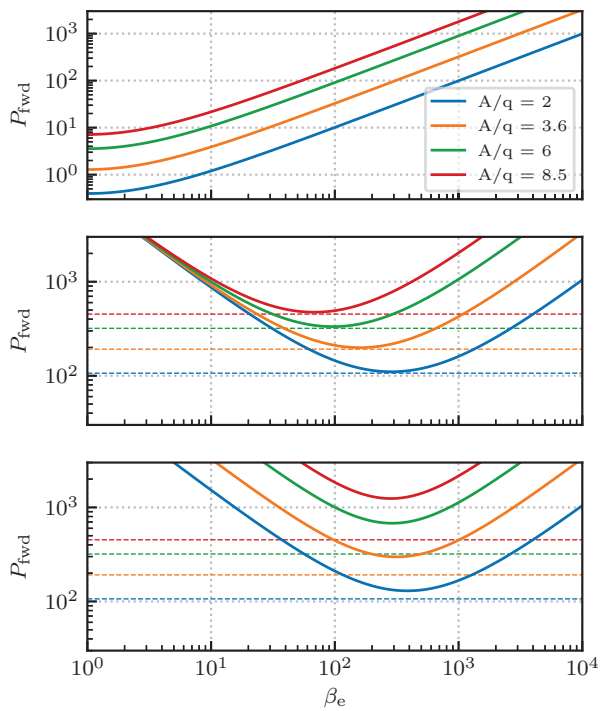

Figure 8: Required forward power to drive CH0 as function of β_e. Top to bottom: $I_{beam} = 0$; $I_{beam} = 100\,\mu A$; $I_{beam} = 100\,\mu A$ and 30 Hz detuning. Dashed, horizontal lines indicate the amount of power transferred to the beam P_{beam}.

ISBN: 978-3-95450-211-0 doi:10.18429/JACoW-SRF2019-MOP081

100 µA was considered. Best matching is now achieved with $\beta_e = 100 - 300$. Since cavity wall losses are small compared to the gain in beam power, the respective best match would require little more power than the fraction which is transferred to the beam. It is obvious, that a universal matching is not possible, since the minimum required power occurs at different β_e for different voltages. The third plot considers a peak detuning of 30 Hz. A choice of a too low β_e now clearly becomes unfavourable.

Figure 9 shows the maximum detuning which can be compensated for by the available RF power (assumed as $P_{max} = 3$ kW) as a function of β_e. The uppermost plot assumes cavity parameters as given in Table 2 and a beam of 100 µA with a synchronous phase of −20°. The center plot shows the curves for reduced Q_0. It reveals the dependency of the β_e with the maximum allowed detuning on Q_0. An over estimation of Q_0 during selection of β_e is dangerous, especially for higher gradients. The lower plot makes clear, that even a reduction of beam current to 30 % does not shift the optimal β_e relevantly.

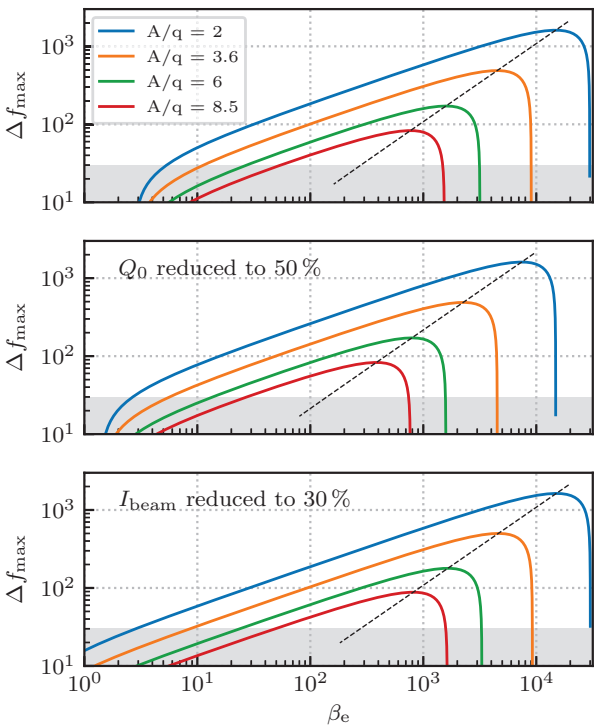

Figure 9: Maximum detuning Δf_{max} of CH0 which can be compensated for by the available forward power (3 kW). The shaded area marks the expected peak level of microphonic detuning. Dashed lines indicate the maximum Δf_{max} as function of the cavity voltage.

Figure 10 shows an equivalent set of plots for the 2-gap re-buncher cavity. While the effect of beam-loading is considerably reduced, because there is nearly no net acceleration applied to the beam (synchronous phase of $\phi_s = -88°$ assumed), compensation of microphonic detuning still shifts the optimal β_e to values around 300. The third plot considers a peak detuning of 60 Hz, since simulations indicate a higher sensitivity compared to CH0.

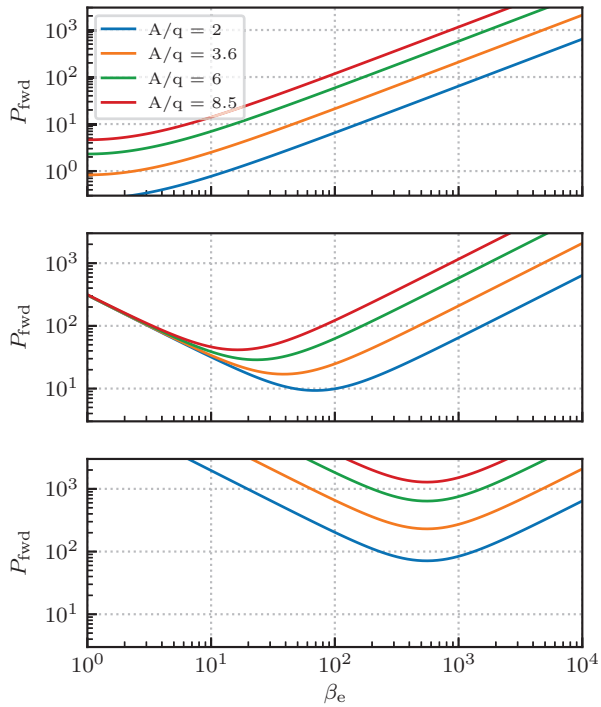

Figure 10: Required forward power to drive re-buncher B1 as function of β_e. Top to bottom: $I_{beam} = 0$; $I_{beam} = 100$ µA; $I_{beam} = 100$ µA and 60 Hz detuning. The amount of power transferred to the beam P_{beam} is nearly zero.

Figure 11 again shows the maximum detuning which can be compensated for by a given maximum available forward power of $P_{fwd} = 3$ kW, but this time for the re-buncher cavity. An assumed reduction in Q_0 has a similar effect like for the accelerating cavity CH0. Naturally, a change in beam current does not play any role in the choice of the optimal β_e.

Summing up, the power couplers of both cavities, B1 and CH0, should be setup with $\beta_e \approx 300$ to 1000. Deviation from this range should be well-founded and requires a precise knowledge about the expected amount of microphonic detuning.

Optimal Detuning

The examination described above assumed the cavity was driven on resonance. This leads to suboptimal utilization of the forward power. The off-crest accelerated beam current causes the impedance of the cavity-beam-system to have a non-real component. As a result, the amplifier has to provide additional reactive power. This can be compensated for, by driving the cavity slightly off-resonance. If done properly, the RF amplifier will not see any reactive load anymore. Table 3 compares the power required for acceleration of different beam currents for $\phi_s = -30°$. The achieved savings of about 3 % are not relevant at an overall power level of about

ISBN: 978-3-95450-211-0 doi:10.18429/JACoW-SRF2019-MOP081

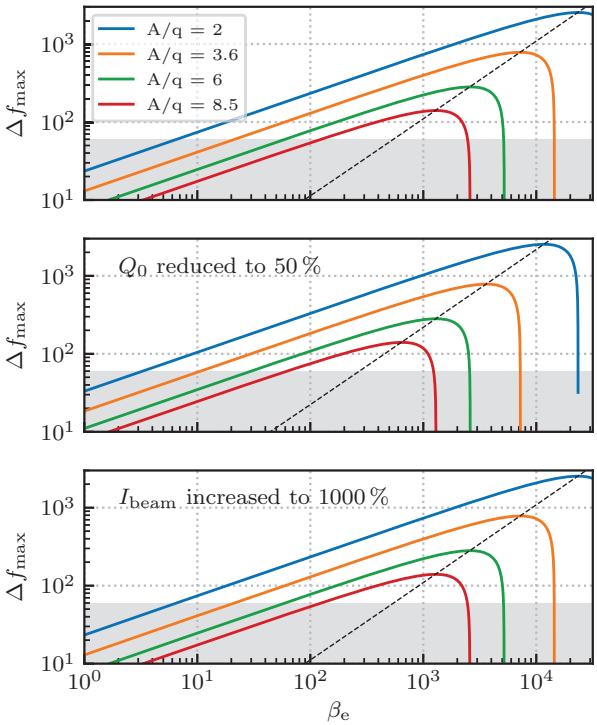

Figure 11: Maximum detuning Δf_{max} of re-buncher B1 which can be compensated for by the available forward power (3 kW). The shaded area marks the expected peak level of microphonic detuning. Dashed lines indicate the maximum Δf_{max} as function of the cavity voltage.

3 kW and do not justify the application of this compensation technique.

Table 3: Reduction of Power Requirements for Correctly Detuned Cavity ($A/q = 6$; Microphonics Neglected)

I_{beam}	P_{beam}	$P_{fwd,off-resonance}/P_{fwd,on-resonance}$
0 µA	0 W	3.6 W/3.6 W = 100%
10 µA	29 W	35.5 W/36.5 W = 97%
100 µA	294 W	323 W/334 W = 97%
1 mA	2944 W	3199 W/3304 W = 97%

ACTIVE MICROPHONICS CANCELLATION

Figure 12 shows the maximum beam current which can be accelerated for given β_e and amplifier power $P_{max} = 3$ kW as function of the peak detuning. As the comparison of the β_e-equals-800 and β_e-equals-1200 curves show, a reduction in peak detuning (Δf) below 100 Hz does not allow for a substantial increase in the maximum beam current. Therefore, while a fast piezo-based frequency tuner has been designed and characterized on the bench [21], there is no urgent need to utilize it for the *Advanced CW-Linac Demonstrator*. Nevertheless, the active cancellation of microphonics could still

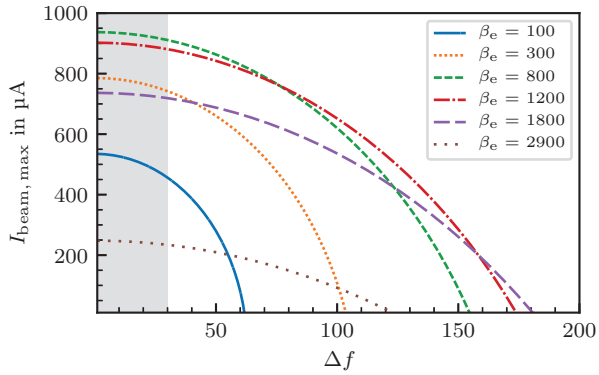

Figure 12: Maximum beam current as function of peak detuning for different β_e for CH0 with $A/q = 6$. The shaded area marks the expected peak level of microphonic detuning.

be of interest, if the beam current is increased or the microphonic disturbances in the new cryomodule are stronger than expected today.

CONCLUSION

The choice of coupling influences the required forward power significantly. Both Q_0 and the expected amount of microphonic need to be carefully considered. Characterization of the microphonics of each individual resonator in its respective final position inside the cold-string is advisable. Driving the cavity off-resonance is not required for low currents and ϕ_S relatively close to zero, but might be worth further investigation when the acceleration of beam currents higher than 100 µA at ϕ_S farther from zero is desired.

While the cavities will always be operated in CW-mode, the beam might still show a pulsed scheme for many modes of operation. Therefore, future work will also need to analyze the effect of transient behaviour.

REFERENCES

[1] W. Barth *et al.*, "High brilliance uranium beams for the GSI FAIR", *Phys. Rev. Accel. Beams*, vol. 20, p. 050 101, 5 2017. DOI: 10.1103/PhysRevAccelBeams.20.050101.

[2] J. Khuyagbaatar *et al.*, "^{48}Ca +^{249} Bk fusion reaction leading to element $Z = 117$: Long-lived α-decaying ^{270}Db and discovery of ^{266}Lr", *Phys. Rev. Lett.*, vol. 112, p. 172 501, 17 2014. DOI: 10.1103/PhysRevLett.112.172501.

[3] F. D. Dziuba *et al.*, "First performance test on the superconducting 217 MHz CH cavity at 4.2 K", in *Proc. of LINAC2016*, 2016, pp. 953–955. DOI: 10.18429/JACoW-LINAC2016-THPLR044.

[4] F. D. Dziuba *et al.*, "First cold tests of the superconducting CW demonstrator at GSI", in *Proc. of RUPAC2016*, 2016, pp. 84–86. DOI: 10.18429/JACoW-RUPAC2016-WECBMH01.

[5] W. Barth *et al.*, "First heavy ion beam tests with a superconducting multigap CH cavity", *Phys. Rev. Accel. Beams*, vol. 21, p. 020 102, 2 2018. DOI: 10.1103/PhysRevAccelBeams.21.020102.

ISBN: 978-3-95450-211-0 doi:10.18429/JACoW-SRF2019-MOP081

[6] W. Barth *et al.*, "A superconducting CW-linac for heavy ion acceleration at GSI", *EPJ Web Conf.*, vol. 138, p. 01 026, 2017. DOI: 10.1051/epjconf/201713801026.

[7] W. Barth *et al.*, "Superconducting CH-cavity heavy ion beam testing at GSI", *J. Phys. Conf. Ser.*, vol. 1067, p. 052 007, 2018. DOI: 10.1088/1742-6596/1067/5/052007.

[8] M. Miski-Oglu *et al.*, "Beam commissioning of the demonstrator setup for the superconducting continuous wave HIM/GSI-linac", in *Proc. IPAC'19*, paper MOZZPLM1, 2019, unpublished.

[9] M. Schwarz *et al.*, "Beam dynamics simulations for the new superconducting CW heavy ion LINAC at GSI", *J. Phys. Conf. Ser.*, vol. 1067, p. 052 006, 2018. DOI: 10.1088/1742-6596/1067/5/052006.

[10] M. Gusarova, W. A. Barth, M. Miski-Oglu, M. Basten, M. Busch, and S. Yaramyshev, "Design of the two-gap superconducting re-buncher", in *Proc. of IPAC2018*, 2018, pp. 2779–2782. DOI: doi:10.18429/JACoW-IPAC2018-WEPML039.

[11] J. List *et al.*, "High power coupler R&D for superconducting CH-cavities", in *Proc. LINAC'18*, 2018, pp. 920–923. DOI: 10.18429/JACoW-LINAC2018-THPO107.

[12] J. List *et al.*, "Modular power couplers for 217 MHz superconducting CH-cavities", in *Proc. of SRF2019*, 2019, paper MOP050, this conference.

[13] F. D. Dziuba *et al.*, "Further RF measurements on the superconducting 217 MHz CH demonstrator cavity for a CW linac at GSI", in *Proc. IPAC'19*, paper WEPRB014, 2019, unpublished.

[14] F. Dziuba *et al.*, "Development of superconducting crossbar-*H*-mode cavities for proton and ion accelerators", *Phys. Rev. ST Accel. Beams*, vol. 13, p. 041 302, 4 2010. DOI: 10.1103/PhysRevSTAB.13.041302.

[15] M. Busch *et al.*, "Overview on SC CH-cavity development", in *Proc. IPAC'19*, paper WEPRB012, 2019, unpublished.

[16] F. D. Dziuba *et al.*, "Structural, mechanical and rf measurements on the superconducting 217 MHz CH cavity for the CW demonstrator at GSI", in *Proc. of IPAC2015*, 2015, pp. 3730–3732. DOI: 10.18429/JACoW-IPAC2015-THPF021.

[17] S. Minaev, U. Ratzinger, H. Podlech, M. Busch, and W. Barth, "Superconducting, energy variable heavy ion linac with constant β, multicell cavities of CH-type", *Phys. Rev. ST Accel. Beams*, vol. 12, p. 120 101, 12 2009. DOI: 10.1103/PhysRevSTAB.12.120101.

[18] S. Yaramyshev *et al.*, "Advanced approach for beam matching along the multi-cavity SC CW linac at GSI", *J. Phys. Conf. Ser.*, vol. 1067, p. 052 005, 2018. DOI: 10.1088/1742-6596/1067/5/052005.

[19] M. Schwarz *et al.*, "Advanced beam dynamics design for the superconducting heavy ion accelerator HELIAC", in *Proc. IPAC'19*, paper MOPTS034, 2019, unpublished.

[20] P. B. Wilson and J. E. Griffin, "High energy electron linacs; application to storage ring RF systems and linear colliders", in *AIP conference proceedings*, vol. 87, 1982. DOI: 10.1063/1.33620.

[21] M. Amberg *et al.*, "The fast piezo-based frequency tuner for SC CH-cavities", in *Proc. LINAC'14*, 2014, pp. 214–216, paper MOP050.